International Journal of Minerals, Metallurgy and Materials
Volume 25, Number 2, February 2018, Page 131
https://doi.org/10.1007/s12613-018-1556-0

A method for recovery of iron, titanium, and vanadium from vanadium-bearing titanomagnetite

Yi-min Zhang[1,2,3)], *Li-na Wang*[2,3)], *De-sheng Chen*[2,3)], *Wei-jing Wang*[2,3)], *Ya-hui Liu*[2,3)], *Hong-xin Zhao*[2,3)], *and Tao Qi*[2,3)]

1) University of Chinese Academy of Sciences, Beijing 100049, China

2) National Engineering Laboratory for Hydrometallurgical Cleaner Production Technology, Beijing 100190, China

3) Key Laboratory of Green Process and Engineering, Institute of Process Engineering, Chinese Academy of Sciences, Beijing 100190, China

(Received: 21 February 2017; revised: 15 June 2017; accepted: 19 June 2017)

Abstract: An innovative method for recovering valuable elements from vanadium-bearing titanomagnetite is proposed. This method involves two procedures: low-temperature roasting of vanadium-bearing titanomagnetite and water leaching of roasting slag. During the roasting process, the reduction of iron oxides to metallic iron, the sodium oxidation of vanadium oxides to water-soluble sodium vanadate, and the smelting separation of metallic iron and slag were accomplished simultaneously. Optimal roasting conditions for iron/slag separation were achieved with a mixture thickness of 42.5 mm, a roasting temperature of 1200°C, a residence time of 2 h, a molar ratio of C/O of 1.7, and a sodium carbonate addition of 70wt%, as well as with the use of anthracite as a reductant. Under the optimal conditions, 93.67% iron from the raw ore was recovered in the form of iron nugget with 95.44% iron grade. After a water leaching process, 85.61% of the vanadium from the roasting slag was leached, confirming the sodium oxidation of most of the vanadium oxides to water-soluble sodium vanadate during the roasting process. The total recoveries of iron, vanadium, and titanium were 93.67%, 72.68%, and 99.72%, respectively.

Keywords: recovery; vanadium; titanomagnetite; direct reduction; sodium oxidation; smelting separation; water leaching

1. Introduction

Vanadium-bearing titanomagnetite is a strategic source of titanium, vanadium, iron, and other valuable elements [1–2]. In China, the Panzhihua-Xichang (Panxi) district is widely recognized as the largest deposit of vanadium-bearing titanomagnetite, with future reserves of 3×10^{10} t, accounting for 75wt% of the entire nation's reserves [3–4]. Hence, the development of methods to effectively utilize the vanadium-bearing titanomagnetite in the Panxi district would be beneficial.

Three technological processes are currently used to separate and recover valuable elements from vanadium-bearing titanomagnetite. One is the blast-furnace process [5–6], where sintered or pelletized titanomagnetite is smelted in a blast furnace to obtain molten iron and blast furnace slag. More than 3×10^6 t of blast furnace slag containing 22wt%–25wt% TiO_2 is produced every year in China [2,7]. However, thus far, the slag has not been efficiently utilized because of its scattered distribution of titanium components in various fine-grained mineral phases with complex interfacial combinations, resulting in the waste of valuable resources as well as in adverse environmental effects [8–9]. Furthermore, the recoveries of iron and vanadium are 70% and 47%, respectively, which are not satisfactory.

The second process is the direct reduction–electric furnace smelting separation process [10-12], where titanomagnetite is successively pelletized, preliminarily reduced in a rotary hearth furnace, and smelted in an electric furnace for removal of titanium slag from vanadium-bearing molten iron. Semi-steel and vanadium slag are obtained by oxidizing the molten iron in a basic oxygen furnace converter [13]. The vanadium components in the vanadium slag are usually transformed into water-soluble sodium metavanadate by so-

Corresponding author: Tao Qi E-mail: tqgreen@home.ipe.ac.cn

dium salt roasting for recovery of vanadium [8]. However, multi-stage roasting is usually used to enhance the vanadium conversion, resulting in an increase in energy consumption [8]. Moreover, the recoveries of iron, vanadium, and titanium are 77%, 53%, and 0%, which are not substantially higher than the recoveries achieved by the blast-furnace process.

The third method is the direct reduction–magnetic separation process proposed by our laboratory [14]. In this process, titanomagnetite is first reduced using pulverized coal, followed by the removal of powdery iron from the vanadium-bearing titanium tailing by magnetic separation. The vanadium-bearing titanium tailing is leached with hydrochloric acid to produce vanadium-bearing lixivium and titanium-bearing residue. Although the recoveries of iron, vanadium, and titanium are improved greatly using this method, the generation of a large amount of spent acid leads to environmental pollution.

Hence, the development of a cleaner and low-energy-consumption method for the recovery of valuable components from vanadium-bearing titanomagnetite is needed. In the present work, an innovative process is proposed and investigated. This process consists of single-step roasting and single-step water leaching. In the roasting process at relatively lower temperatures (<1200°C), a mixture of ore, reductant, and sodium salt is successively reduced, carburized, smelted, and layered for the difference in density between the molten slag and iron. Iron nuggets are directly separated from the vanadium-bearing titanium slag after natural cooling. The mechanism and influencing factors associated with the removal of iron nuggets from the vanadium-bearing titanium slag during the roasting process were systematically investigated. Behaviors such as slag melting, iron melting, and molten iron and slag separation were observed *in situ*. In addition, the recovery of vanadium by the water leaching process was also investigated. We speculate that the proposed separation method for iron, vanadium, and titanium from vanadium-bearing titanomagnetite could represent a new alternative method for the comprehensive utilization of vanadium-bearing titanomagnetite.

2. Experimental

2.1. Materials and reagents

Vanadium-bearing titanomagnetite concentrates were obtained from the Panxi region, China. The phase compositions, chemical compositions, and mineralogy of the concentrates were investigated in our previous work [15]. Pulverized coal was used as the reductant in the present work. The results of the industrial analyses performed on the various coals used in this work are shown in Table 1. All chemicals were of analytical grade (Sinopharm Chemical Reagent Beijing Co., Ltd.). Demineralized water was used throughout the experiments.

Table 1. Industrial analysis results for various coals wt%

Reductant	Moisture	Ash	Volatile	Fixed carbon
Anthracite	2.08	8.65	3.98	85.29
Graphite	0.16	0.87	2.09	96.88
Bitumite	6.12	22.10	26.74	45.04
Lignite	7.39	5.65	37.12	49.84

2.2. Experimental procedures

2.2.1. Roasting of vanadium-bearing titanomagnetite

In a typical roasting experiment, 50 g of vanadium-bearing titanomagnetite concentrates, with an average particle size of <150 μm, was mixed homogeneously with specific amounts of pulverized coal and a sodium salt. In the powder mixtures, the molar ratio of the fixed carbon in the coal to the reducible oxygen in the concentrates (C/O) was varied within a specified range. The mass ratio of the sodium carbonate to the concentrates was also varied within a specified range. Each mixture was placed into a silicon carbide crucible obtained from the Jinda crucible factory in China. Subsequently, an electric muffle furnace (CNT furnace factory, China) equipped with a temperature control system (±5°C) was heated to the desired temperature in the range from 1150 to 1200°C. The sealed crucible was then placed within the furnace, and an isothermal process was performed for the desired time; the crucible was then removed from the furnace. After the sample was cooled under the protection of nitrogen, the obtained iron nugget was analyzed by chemical methods. To evaluate the quality of the slag–iron smelting separation during the roasting process, we define the iron recovery R by the following equation:

$$R = \frac{M_{\mathrm{n}}}{M_{\mathrm{r}}} \times 100\%,$$

where M_{n} and M_{r} are the mass of iron in the iron nugget and the mass of iron in the raw ore, respectively.

2.2.2. Water leaching of roasting slag

The roasted slag was ground to 90wt% passing 74 μm before being leached. The samples were leached in 50 mL of deionized water at a stirring speed of 300 r/min at 90°C for various time periods. The slurry was then filtrated using a Büchner funnel to obtain the leach liquor and solid residues.

The extractions of vanadium and titanium were calculated by the following formula [16]:

$$X = \left[1 - \left(\frac{C_i}{C} \times \frac{m_i}{m}\right)\right] \times 100\% ,$$

where X is the leaching efficiency of vanadium or titanium; C_i and C are the mass fractions of vanadium or titanium in the leaching residues and in the raw ore, respectively; and m_i and m are the mass of the leaching residues and the raw ore, respectively.

2.3. Chemical analysis

The chemical compositions of the iron nuggets, roasting slag, and the water leaching residue were determined by inductively coupled plasma–atomic emission spectroscopy (ICP–AES, Optima 5300DV, Perkin Elmer, USA). Standard procedures were used to prepare the samples for ICP analysis.

2.4. X-ray diffraction (XRD) analysis

X-ray powder diffraction data were collected on a Bruker D8 Advance automatic diffractometer in the Bragg–Brentano geometry and were used to determine the crystal phases of the raw ore, milled iron nuggets, roasting slag, and the water leaching residue. Cu $K_{\alpha 1}$ radiation (λ = 0.15406 nm) was used with a fixed counting time of 8 s in the range of $5° \leq 2\theta \leq 90°$ with steps of 0.03° in 2θ. Standard procedures were used to prepare the samples for XRD [17].

2.5. X-ray photoelectron spectroscopy (XPS) analysis

XPS analysis of the raw ore and the roasting slag was carried out on an ESCALAB 250Xi electrostatic spectrometer (Thermo Fisher Scientific) equipped with an Al $K_{\alpha 1,2}$ (hv = 1486.6 eV) radiation source; the spectra were collected under a vacuum of 5×10^{-7} Pa at room temperature. The error in the determination of the binding energy and the peak widths did not exceed ±0.1 eV; the error in the relative peak intensity was ±10%. Fitting of the V 2p spectra was essential for determining the oxidation states of V present in the raw ore and in the roasting slag. The fitting was performed on the XPSPEAK 4.1 software after Shirley background subtraction using a Gaussian–Lorentzian sum function.

2.6. SEM investigation

The scanning electron microscopy–energy-dispersive X-ray spectroscopy (SEM–EDS) analysis of sections of the roasting slag and leaching residue was performed using an FEI Quanta 650 environmental scanning electron microscope equipped with a Bruker Quantax 200 dual silicon-drift energy-dispersive X-ray spectrometer. To observe the cross-sectional morphology of the particles, the samples were mounted using Bakelite polymer followed by being ground and polished with 0.5-μm polishing paper [18]. After being polished and cleaned, each sample was carbon coated before SEM examination [19].

2.7. *In situ* observation of the slag/iron smelting separation process

The mixture of vanadium-bearing titanomagnetite, sodium carbonate, and anthracite powder, in which the C/O molar ratio and added sodium carbonate content were 1.7 and 70wt%, respectively, was roasted for 110 min. The obtained roasted product was microscopically observed *in situ* with a confocal laser-scanning microscope combined with an infrared image-heating furnace [20]. The tablet sample was placed in a platinum crucible (outer diameter: 5.0 mm; inner diameter: 4.5 mm; height: 5 mm). The crucible was subsequently placed in the sample chamber of the infrared image-heating furnace located just beneath the laser microscope. During these experiments, the interior of the chamber was maintained under an inert gas atmosphere of highly pure argon flowing at 200 mL/min. The sample was heated to 1100°C at a rate of 1000°C/min. The sample was then continuously heated to 1200°C at a rate of 20°C/min.

3. Results and discussion

3.1. Recovery of iron by the iron nugget forming process

3.1.1. Effect of reductant and sodium salt types

The influence of various types of coals on the iron nugget forming process was investigated. The results show that, among the selected reductants used in this work, including bitumite, anthracite, lignite, and graphite, iron nuggets are only produced during the roasting process when bitumite or anthracite is used as a reductant. As shown in Table 2, although the iron grades in the iron nuggets exhibit little difference, the iron recovery is much greater when anthracite is used as a reductant than when bitumite is used, which indicates that the slag and iron can be separated more effectively during the roasting process when anthracite is used as a reductant. According to the results of the industrial analysis performed on the four types of coal, shown in Table 1, the ash contents of both the anthracite and bitumite are greater than those of the lignite and graphite. Moreover, the ash in the reductant, along with the impurity oxides in the vanadium-bearing titanomagnetite, would finally contribute to the slag formation. Therefore, it is speculated that appropriate ash content within the reductant is favorable for the ef-

fective separation of the molten slag and iron during the roasting process. Additionally, compared with the bitumite, the anthracite contains more carbon, which promotes complete reduction of the iron oxides in the vanadium-bearing titanomagnetite, which is a prerequisite for slag–iron smelting separation [21]. Consequently, anthracite was selected as a reductant in subsequent studies.

Table 2. Effect of various coals on the slag–iron smelting separation process*

Reductant	Iron recovery / %	Iron grade / %
Bitumite	12.68	95.26
Anthracite	93.67	95.48

*Note: roasting temperature, 1200°C; Na_2CO_3 addition, 70wt%; molar ratio of C/O, 1.7; residence time, 2 h.

On the basis of previous studies, four kinds of sodium salts (sodium chloride, sodium sulfate, sodium hydroxide, and sodium carbonate) were used for sodium oxidation of vanadium oxides during the reduction process of vanadium-bearing titanomagnetite [22–26]. According to the experimental results, iron nugget production was only successful when sodium hydroxide or sodium carbonate was added to the roasting system; these results indicate that, compared with sodium chloride and sodium sulfate, sodium hydroxide and sodium carbonate are more effective for the separation of the slag and iron. Furthermore, as shown in Table 3, the iron recovery and iron grade in the iron nuggets in the presence of sodium carbonate is higher than that of sodium hydroxide. This result is attributed to the fact that sodium carbonate and sodium hydroxide decompose to form sodium oxide at the roasting temperature, whereas sodium chloride and sodium sulfate cannot. Sodium oxide can react with the slag phase in the raw ore to form low-melting-point compounds [21]. These low-melting-point materials appear in the form of a liquid phase during the course of reduction, which is beneficial for the diffusion and aggregation of the metallic iron [27]. Additionally, the separation of iron and slag was not clear in the presence of sodium hydroxide and the entrapment of slag in the iron nuggets was directly observed in the cooled roasted products, which is the direct reason for the lower iron grade in the iron nuggets. An underlying reason might be that water formed through dissociation of sodium hydroxide leading to a decrease in the surface tension of the molten slag, which is not beneficial to the smooth separation of slag and iron [28]. Consequently, sodium carbonate was selected for use in subsequent experiments.

Table 3. Effect of various sodium salts on the slag–iron smelting separation process*

Sodium salt	Iron recovery / %	Iron grade / %
NaOH	24.56	84.32
Na_2CO_3	39.67	94.59

*Note: roasting temperature, 1200°C; Na_2CO_3 addition, 50wt%; molar ratio of C/O, 1.7; mixture thickness, 68 mm; residence time, 2 h.

3.1.2. Effect of roasting temperature and residence time

The effect of roasting temperature on the slag–iron smelting separation process is shown in Fig. 1. The results reveal that the slag–iron smelting separation did not occur until the roasting temperature was increased to 1150°C, where the iron recovery and iron grade in the iron nuggets were 10.07% and 80.01%, respectively. As the roasting temperature was increased to 1200°C, the iron recovery and iron grade in the iron nuggets increased to 56.49% and 85.49%, respectively. However, the iron recovery slightly increased to 58.01% and the iron grade in the iron nuggets decreased to 82.38% when the roasting temperature was increased to 1250°C. Obviously, increasing the roasting temperature in the temperature range below 1200°C could promote the formation process of iron nuggets which includes the reduction of iron oxides, carbonization of metallic iron, and the separation of molten slag and molten iron. The process of $Fe_2O_3 \rightarrow Fe_3O_4 \rightarrow FeO$ appears to occur mainly at temperatures under 1000°C, whereas the process of $FeO \rightarrow Fe$ appears to mainly occur at 1000–1100°C, and the whole process is finished at 1200°C [29]. At 1000°C, the carbonization of metallic iron begins [30]. As the temperature increases, the iron oxides are gradually reduced and the metallic iron content increases, which increases the contact area between the metallic iron and carbon, which in turn enhances the carbonization reaction [31]. The higher temperature benefits the melt, the integration of slag, and the integration of iron grains. Larger iron particles will improve the degree of dissociation of iron and slag, leading to an increase in interfacial tension between iron and slag, thereby facilitating their separation [32]. However, when the roasting temperature is greater than 1200°C, vanadium is easily reduced and subsequently dissolves in the molten iron in the presence of excess carbonaceous reductants [14,33]. This process is not favorable for the removal of impurities from iron nuggets or for the comprehensive utilization of vanadium-bearing titanomagnetite. Consequently, a roasting temperature of 1200°C was determined to be optimal for the multipurpose utilization of vanadium-bearing titanomagnetite.

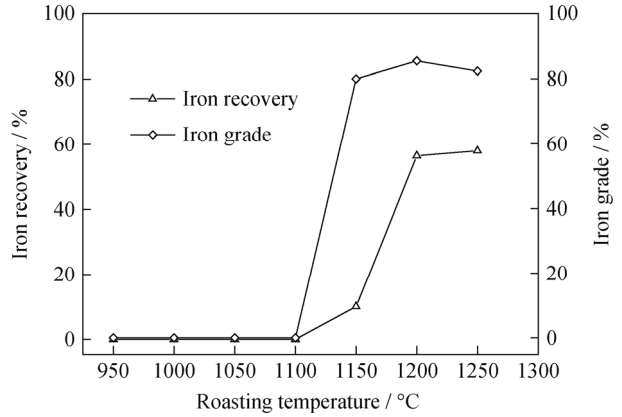

Fig. 1. Effect of roasting temperature on the slag–iron smelting separation process (Na_2CO_3 addition, 60wt%; molar ratio of C/O, 1.5; mixture thickness, 68 mm; residence time, 2 h).

The effect of residence time on the slag–iron smelting separation process was investigated. The results, which are shown in Fig. 2, reveal that iron nuggets were not produced until the residence time was extended to 2 h. Moreover, the iron recovery and iron grade in the iron nuggets remained constant as the residence time was further extended. These results indicate that the iron nugget formation process, including the reduction of iron oxides, carbonization of metallic iron, and slag–iron separation, will be finished when the residence time is 2 h or longer. Thus, a residence time of 2 h is optimal.

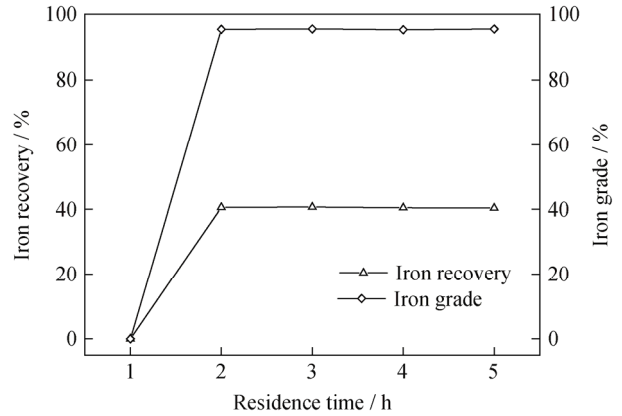

Fig. 2. Effect of residence time on the slag–iron smelting separation process (roasting temperature, 1150°C; Na_2CO_3 addition, 50wt%; molar ratio of C/O, 1.7; mixture thickness, 68 mm).

3.1.3. Effects of the molar ratio of C/O and Na_2CO_3 addition

The effect of the molar ratio of C/O on the slag–iron smelting separation process was investigated; the results are shown in Fig. 3. The iron recovery and iron grade in the iron nuggets first increased and then decreased with the increasing molar ratio of C/O. When the molar ratio of C/O was 1.3, the separation of slag and iron could not be achieved. When it was 1.7, the iron recovery reached a maximum value of 72.18% and the iron grade in the iron nuggets was 95.38%. When the molar ratio of C/O increased to 2.1, iron nuggets did not form, possibly because the C/O molar ratio of 1.7 is a critical value at which iron oxides are reduced thoroughly and the ideal amount of carbon for saturation is dissolved in the molten iron. As the molar ratio of C/O increases within the range from 1.3 to 2.1, the Boudouard reaction proceeds at a higher rate to provide the reductant CO, which increases the ratio of CO/CO_2 and accelerates the reduction process [21]. When the molar ratio of C/O is greater than 1.7, excess carbon is present in the roasting system as a solid, which prevents the molten slag and iron from flowing and aggregating, resulting in the reduction or even the disappearance of iron nuggets [21]. In short, to achieve good separation of slag and iron, a C/O molar ratio of 1.7 is most appropriate.

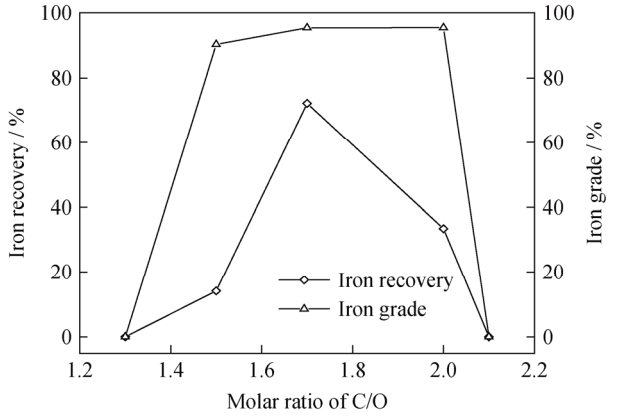

Fig. 3. Effect of the molar ratio of C/O on the slag–iron smelting separation process (roasting temperature, 1200°C; Na_2CO_3 addition, 70wt%; residence time, 2 h; mixture thickness, 68 mm).

The influence of different Na_2CO_3 additions (the mass ratio of Na_2CO_3 to the raw ore) on the smelting separation process was investigated. The experimental results at different Na_2CO_3 additions are shown in Fig. 4. As shown in Fig. 4, both the iron recovery and the iron grade in the iron nuggets first increased and then decreased with increasing Na_2CO_3 addition. When the Na_2CO_3 addition was 40wt%, the separation of slag and iron could not be achieved. When the Na_2CO_3 addition was increased from 50wt% to 70wt%, the iron recovery increased from 39.67% to 72.18% and the iron grade in the iron nuggets increased from 82.26% to 95.38%. When the Na_2CO_3 addition exceeded 70wt%, the iron recovery and iron grade in the iron nuggets tended to decrease and finally approach zero. According to previous studies [21], the solid slag phase increases the distance between the reducing agent and the raw ore fines, which is less

conducive to the reduction, carburizing, gathering, and growth of iron. We therefore speculate that, at 70wt% of Na_2CO_3 addition, nonferrous mineral phases in the raw ore have completely reacted with Na_2CO_3, forming low-melting-point compounds [23]. When the Na_2CO_3 addition was increased within the range of 40wt%–70wt%, chemical reactions involving Na_2CO_3 were promoted and the ratio of the molten slag to non-molten slag subsequently increased. When the Na_2CO_3 addition exceeded 70wt%, excessive Na_2CO_3 was present in the roasting system in the form of liquid, resulting in the inclusion of molten slag on the surface of iron (the surface tension of slag is 0.2–0.4 N/m, and the surface tension of iron is 1.6–1.8 N/m) [34], which inhibited the separation of iron and slag. Consequently, on the basis of the aforementioned results, the recommended Na_2CO_3 addition is 70wt%.

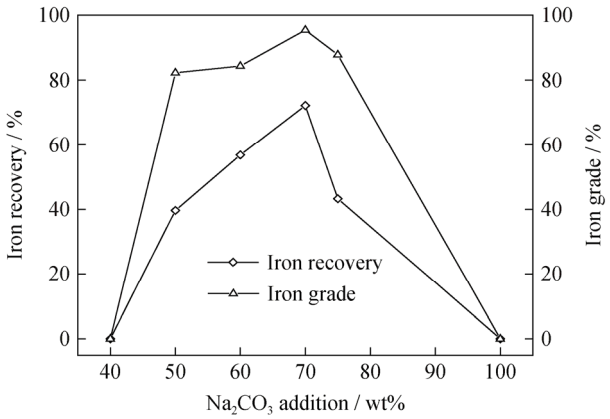

Fig. 4. Effect of sodium carbonate addition on the slag–iron smelting separation process (roasting temperature, 1200°C; molar ratio of C/O, 1.7; residence time, 2 h; mixture thickness, 68 mm).

3.1.4. Determination of slag–iron smelting separation regions

As previously mentioned, the slag–iron smelting separation process was influenced by numerous factors, including the roasting temperature, residence time, and the additions of coal and sodium salts. When the other conditions remain constant, the slag–iron smelting separation process will only occur when the coal and sodium salt additions are individually determined within a certain range. In this section, the smelting separation regions at various roasting temperatures are defined by the amount of anthracite (i.e., the molar ratio of C/O) and the amount of Na_2CO_3 added to the roasting system (i.e., the mass ratio between Na_2CO_3 and the raw ore), which were individually investigated and determined. At a fixed roasting temperature of 1150°C, the effect of the molar ratio of C/O in the range from 1.3 to 2.1 on the smelting separation process was investigated whilst the sodium additions were individually fixed at 40wt%, 50wt%, 60wt%, 70wt%, 75wt%, and 80wt%; the results are shown in Fig. 5.

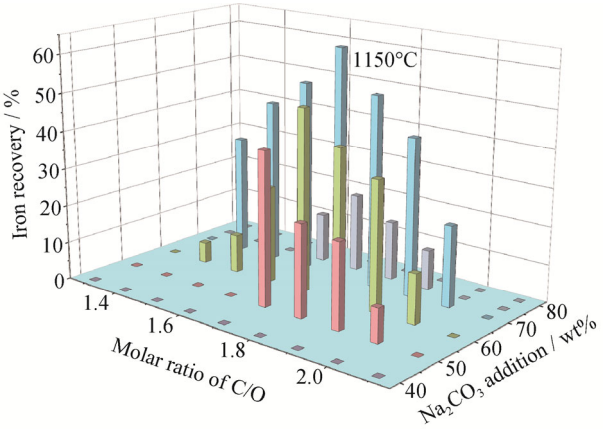

Fig. 5. Slag–iron smelting separation regions considering the molar ratio of C/O and Na_2CO_3 addition at 1150°C.

When the sodium carbonate was fixed at 40wt% or 80wt%, the smelting separation process did not occur, irrespective of the C/O ratio. Obviously, insufficient or excess sodium carbonate is not favorable for the smelting separation process. When the sodium carbonate addition content was individually fixed at 50wt%, 60wt%, 70wt%, or 75wt%, the smelting separation would consistently occur provided that the molar ratio of C/O was a certain value. In addition, as the molar ratio of C/O was increased, the iron recovery consistently presented a parabolic trend. According to the results shown in Fig. 5, if the molar ratio of C/O is fixed at a specific value, the effect of the sodium carbonate addition on the smelting separation process will follow the aforementioned principles. Similarly, when the roasting temperature was fixed at 1200°C, the effect of the molar ratio of C/O on the smelting separation process was investigated while the sodium carbonate addition was individually fixed at 40wt%, 50wt%, 60wt%, 70wt%, 75wt%, or 100wt%. As shown in Fig. 6, the trend is clearly similar to that obtained at a roasting temperature of 1150°C.

The operational flexibility diagram regarding the slag–iron smelting separation process was obtained and is shown in Fig. 7; the iron recovery is disregarded. The smaller region is the region where slag–iron smelting separation will occur at a roasting temperature of 1150°C when both the molar ratio of C/O and the sodium carbonate addition are within the ranges defined in this region. The larger region represents the smelting separation region at a roasting temperature of 1200°C. Obviously, the smelting separation area represented at a roasting temperature of 1200°C is larger than that at 1150°C. Furthermore, the results in Figs.

5–7 lead to two conclusions. First, the iron nuggets are not produced at the boundaries of the two regions. Second, in both regions, the iron recovery increases from the boundary to the center. Consequently, the iron recovery is maximal at the center of each region, which is also optimal with regard to the recovery of the resources.

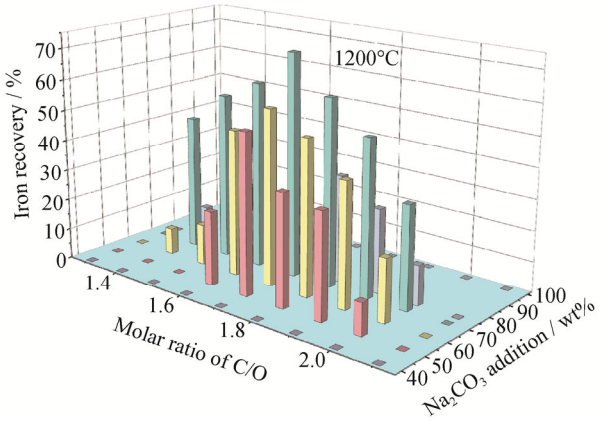

Fig. 6. Slag–iron smelting separation regions considering the molar ratio of C/O and Na_2CO_3 addition at 1200°C.

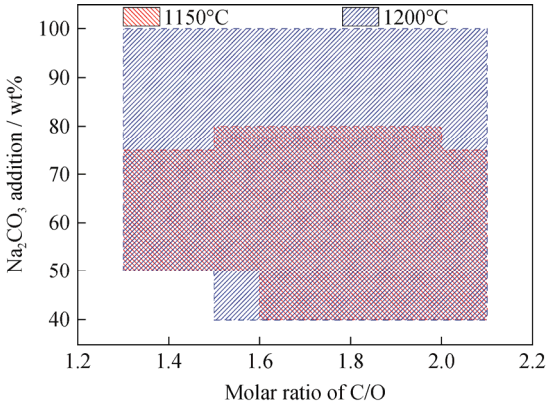

Fig. 7. Operational flexibility diagram for iron nugget production.

3.1.5. Optimal roasting conditions

As detailed in the previous discussion, numerous roasting conditions have been optimized, including the coal type, sodium salt type, roasting temperature, residence time, molar ratio of C/O, and Na_2CO_3 addition. However, the iron recovery is not sufficient. To enhance the iron recovery, we investigated the effect of the mixture thickness on the slag–iron smelting separation process; the results are presented in Fig. 8. As the mixture thickness was decreased from 68.0 to 42.5 mm, the iron recovery increased from 72.18% to 98.15%, and the iron grade in the iron nuggets increased from 90.32% to 95.44%. Obviously, reducing the mixture thickness is beneficial to the slag–iron smelting separation. The mixture thickness represents the total distance the molten iron or molten slag is required to flow. When the other conditions remain unchanged, the decrease in mixture thickness facilitates the aggregation of the molten iron or molten slag and their separation.

Finally, the optimal roasting conditions were obtained: anthracite as the reductant, Na_2CO_3 as the additive, a roasting temperature of 1200°C, a residence time of 2 h, a C/O molar ratio of 1.7, Na_2CO_3 addition of 70wt%, and a mixture thickness of 42.5 mm.

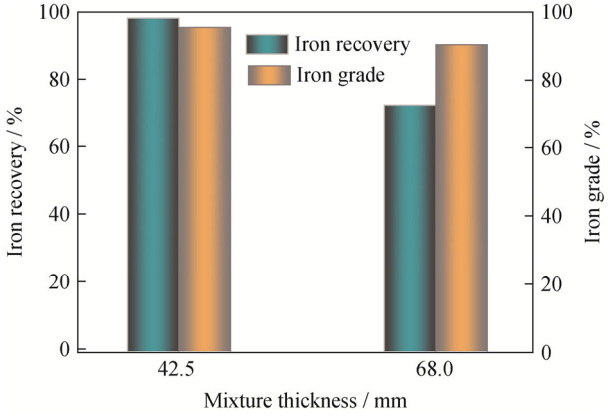

Fig. 8. Effect of the mixture thickness on the slag–iron smelting separation process (roasting temperature, 1200°C; molar ratio of C/O, 1.7; Na_2CO_3 addition, 70wt%; residence time, 2 h).

3.2. Analysis of roasted products

The morphologies of the feed and roasted products obtained under the optimal roasting conditions are shown in Fig. 9, which reveals that well-separated roasting slag and iron nuggets were directly obtained by roasting the powdery

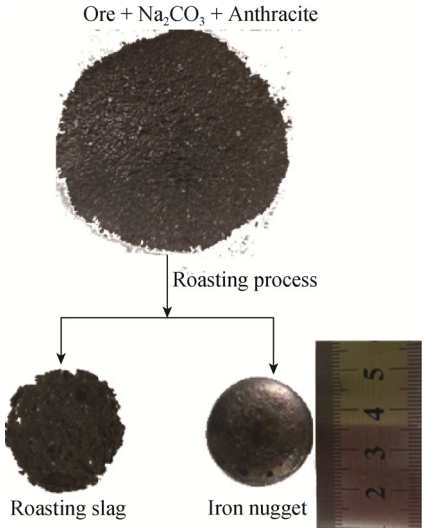

Fig. 9. Morphologies of the feed and roasted products.

mixture including ore, anthracite, and Na_2CO_3. The phase compositions of the raw ore, iron nugget, and roasting slag are presented in Fig. 10. The raw ore is mainly composed of magnetite (Fe_3O_4), ilmenite ($FeTiO_3$), and titanomagnetite ($Fe_{2.75}Ti_{0.25}O_4$). The iron nugget consists of metallic iron, and the roasting slag includes a small amount of $CaTiO_3$ and some complex sodium salts including $Na_{1.74}Mg_{0.865}Si_{1.135}O_4$, $(Na_2O)_{0.33}NaAlSiO_4$, and $Na_{1.74}Mg_{0.79}Al_{0.15}Si_{1.06}O_4$. Additionally, the chemical compositions of an iron nugget and the roasting slag and the distribution ratio of valuable elements in an iron nugget and roasting slag are shown in Tables 4 and 5, respectively. The results show that 93.67wt% iron is concentrated in the iron nugget and that 99.82wt% titanium and 84.9wt% vanadium simultaneously enter the roasting slag. The iron nugget, with an iron content of 95.44wt%, could be directly used in the steelmaking industry. The roasting slag with a titanium content of 12.64wt% and a vanadium content of 0.35wt% was further used to recover vanadium and titanium.

3.3. Recovery of vanadium and titanium

The separation of vanadium and titanium in roasting slag was carried out using a water leaching process. The leaching efficiencies of vanadium and titanium as functions of time are presented in Fig. 11, which reveals that vanadium was gradually leached into the leaching liquor and that titanium remained stable in the leaching residue with increasing leaching time. According to the leaching rate, the leaching of vanadium mainly consists of three steps: fast leaching (0–10 min), slow leaching (10–60 min), and leaching equilibrium (60–120 min). Consequently, 1 h was the optimal leaching time.

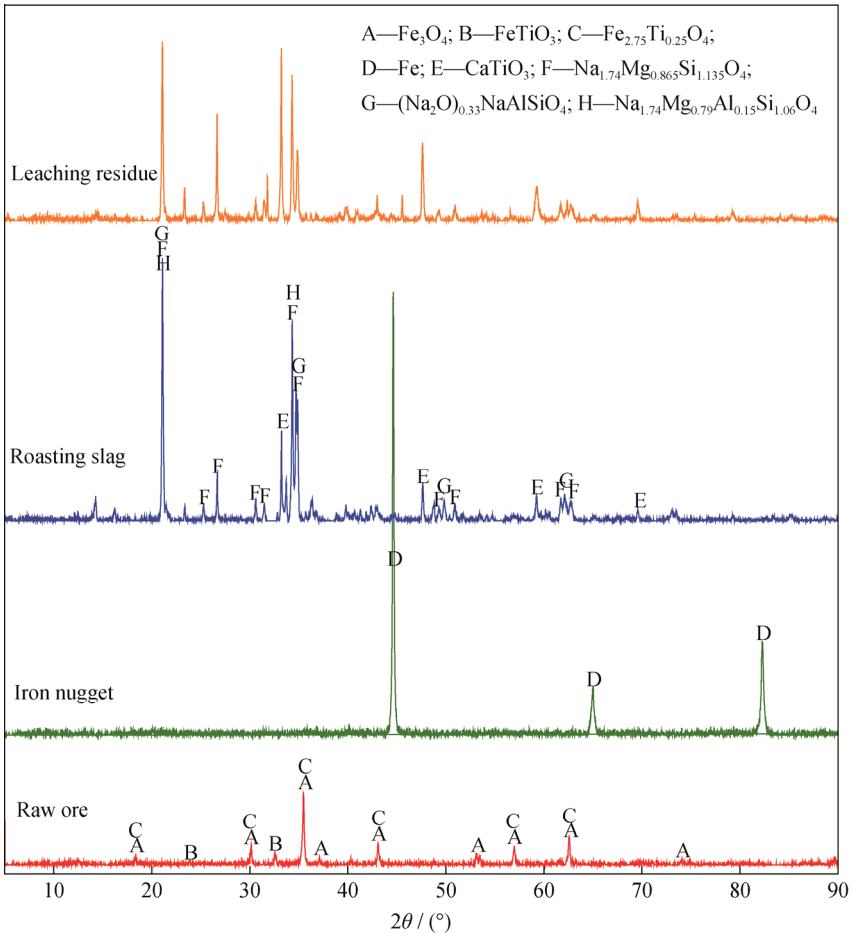

Fig. 10. XRD patterns of different samples.

Table 4. Chemical composition of the samples wt%

Sample	Fe	C	Ti	V	Mn	Ca	Mg	Al	Si	P	S
Iron nugget	95.44	3.08	0.029	0.095	0.096	—	—	—	0.025	<0.005	0.011
Roasting slag	6.03	—	12.64	0.350	0.26	1.48	4.43	5.80	6.74	—	—
Leaching residue	7.27	—	13.22	0.078	0.31	9.86	6.19	8.84	15.06	—	—

Table 5. Distribution ratio of elements in the iron nugget and roasting slag wt%

Sample	Fe	Ti	V
Iron nugget	93.67	0.18	15.1
Roasting slag	6.33	99.82	84.9

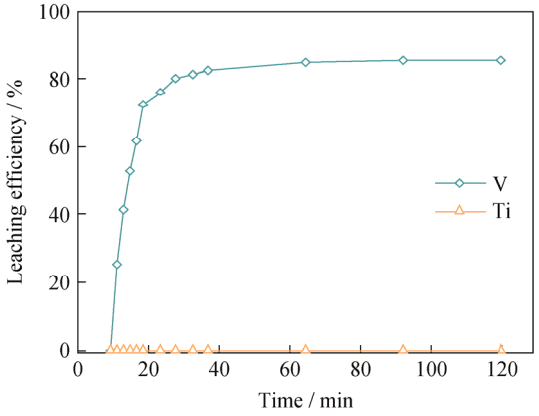

Fig. 11. Leaching efficiencies of vanadium and titanium from the roasting slag as functions of time.

The transfer of vanadium from a solid phase into aqueous solution occurs via the formation of water-soluble sodium vanadate with V(V), which is the result of the sodium oxidation of vanadium oxides from the raw ore during the aforementioned roasting process. To verify this viewpoint, the valences of vanadium in the raw ore and in the roasting slag were confirmed by XPS analysis; the results are shown in Fig. 12. As shown in Fig. 12(a), the vanadium existed in the raw ore mainly in the form of V(III). According to Fig. 12(b), 89.01at% of the vanadium was oxidized to V(V) after the roasting process.

Additionally, the phase compositions and chemical compositions of the leaching residue are presented in Fig. 10 and Table 4, respectively. As shown in Fig. 10, the phase composition of the leaching residue was nearly identical to that of roasting slag except for the slight decrease in the amount of complex sodium salts as a result of their partial dissolution in the aqueous solution. As listed in Table 4, the contents of vanadium in the roasting slag and in the leaching residue were 0.35wt% and 0.078wt%, respectively. Additionally, backscattered electron images of the roasting slag and the leaching residue and elemental mapping images of vanadium are presented in Fig. 13. The amount of vanadium in the solids substantially decreased after the water leaching process. The aforementioned experimental results confirm the transfer of vanadium from the solid to the aqueous solution.

3.4. Proposal of a novel method for multipurpose utilization of vanadium-bearing titanomagnetite and discussion of its novelty

According to the experimental results and aforementioned discussion, a novel method for the recovery of iron, vanadium, and titanium from vanadium-bearing titanomagnetite is proposed. We term this method "direct reduction–sodium oxidation–smelting separation coupled technology", and a flow diagram depicting this process is shown in Fig. 14. First, the vanadium-bearing titanomagnetite powder, sodium salt, and reductant are uniformly mixed. The mixture is subsequently roasted at relatively low temperatures compared with those in a blast furnace or electric furnace. During the roasting process, the direct reduction of iron oxides by carbon, the sodium oxidation of vanadium oxides by sodium salts, and the slag–iron smelting separation are realized successively. Following the roasting process, a well-separated iron nugget with 93.67% iron from the raw ore and a roasting slag with 84.90% vanadium and 99.72% titanium from the raw ore are directly obtained. These iron nuggets could be used to produce semi-steel. After a water leaching process, 85.61% vanadium from the roasting slag can be leached into water leaching liquor and almost all of the titanium is concentrated in the leaching slag.

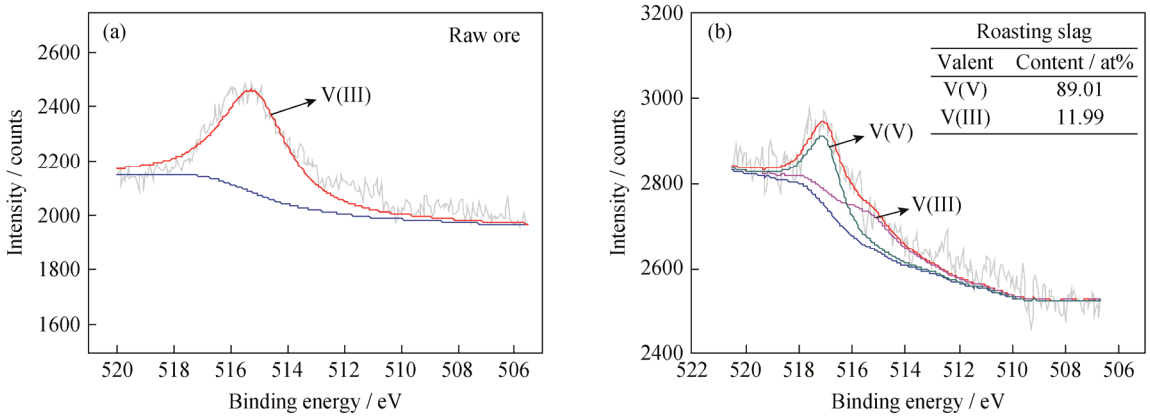

Fig. 12. XPS spectra of V $2p_{3/2}$ of the raw ore (a) and the roasting slag (b).

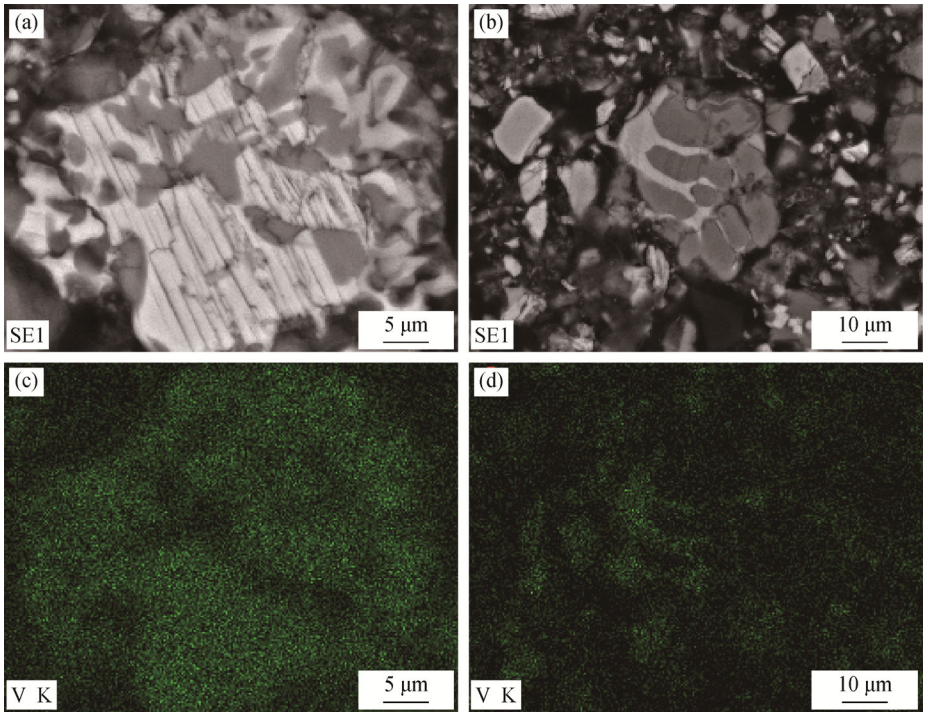

Fig. 13. Backscattered electron images and X-ray maps of vanadium in the roasting slag (a, c) and the leaching residue (b, d).

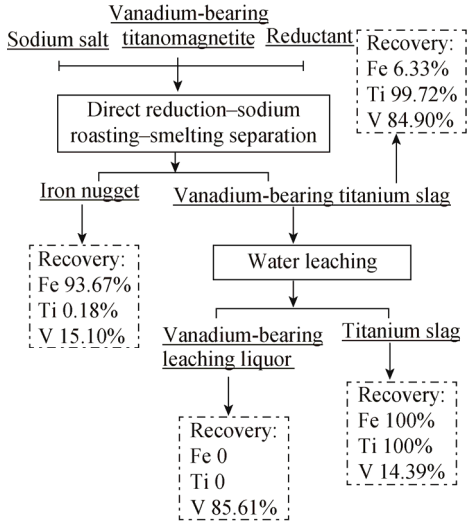

Fig. 14. Flow sheet of the direct reduction–sodium oxidation–smelting separation coupled process.

Compared with traditional methods used for the recovery of valuable elements from vanadium-bearing titanomagnetite, the direct reduction–sodium oxidation–smelting separation coupled technology features three advantages. First, the reduction of iron oxides, the sodium oxidation of vanadium oxides, and the smelting separation of slag–iron can be simultaneously realized during a single-step roasting process at a relatively low roasting temperature. The low temperatures of this process can substantially reduce the energy consumption and operational costs. Second, this novel process enhances the recovery and utilization of iron, vanadium, and titanium from vanadium-bearing titanomagnetite. Third, this novel process is environmentally friendly and does not produce any hazardous substances.

3.5. Mechanism of the iron nugget forming process

A schematic of the iron nugget forming process is shown in Fig. 15. In general, the iron nugget forming generally consists of three steps: the preparation of the mixture, low-temperature roasting, and natural cooling. The ore, coal, and sodium carbonate are mixed uniformly. Subsequently, the mixture is roasted at a relatively low temperature for a specific period. During the roasting process, numerous complex chemical reactions and physical processes occur in succession. Molten iron and molten slag are independently produced. Given the production of molten iron, the iron oxides are initially reduced by carbon. After the iron oxides are thoroughly reduced, a carburization reaction occurs between the metallic iron and excess carbon. Subsequently, the iron particles contain carbon melt. The reactions between sodium carbonate and other oxides such as V_2O_3, Al_2O_3, and SiO_2, as well as the melting of the slag consisting of substances with low melting points, have previously occurred in succession. When the fluidity of the molten slag and molten iron attains a certain level, the molten slag and iron mutually flow and finally separate from each other because of immiscibility and differences in their density. After natural cooling, iron nuggets well separated from the roasting slag are finally obtained.

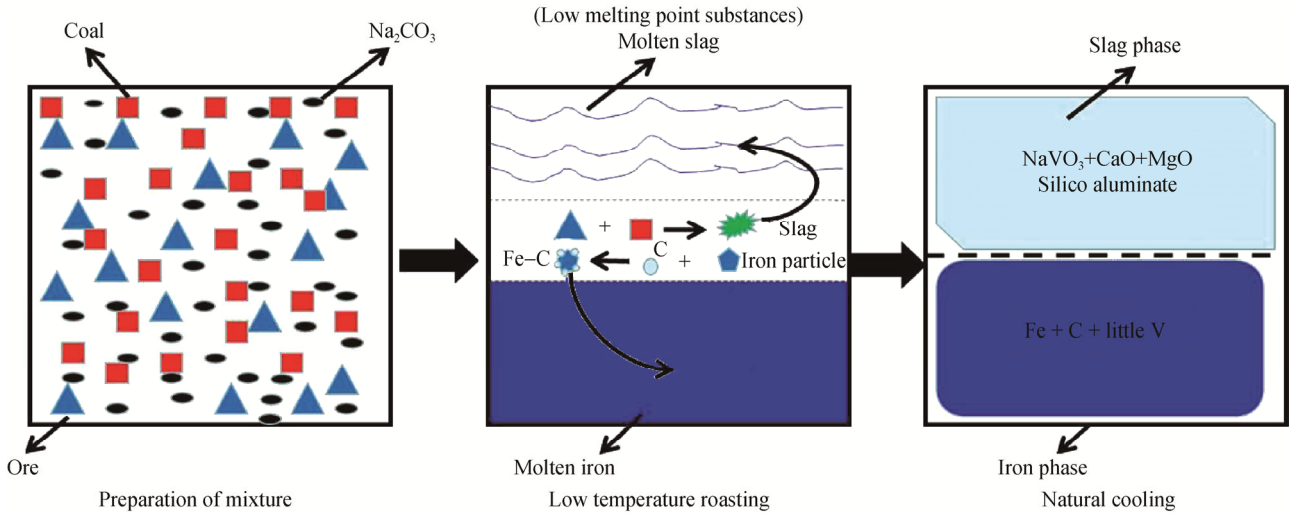

Fig. 15. A schematic of the direct reduction–sodium oxidation–smelting separation process.

3.6. *In situ* observation of the slag–iron smelting separation process

The melting and aggregation processes were observed for the slag and iron; the resultant images are shown in Figs. 16 and 17, respectively. As shown in the figures, the melting and aggregation processes of the slag are similar to those of the iron. These processes primarily consist of four steps: no melting, melting initiation, melting in multiple regions, and flowing and aggregation. As shown in Fig. 18, when the fluidity of the molten iron and molten slag attains a certain level, the molten iron and molten slag flow mutually and separate from each other due to immiscibility and the difference in their densities. The molten iron thus disappears from the area of observation because of its higher density.

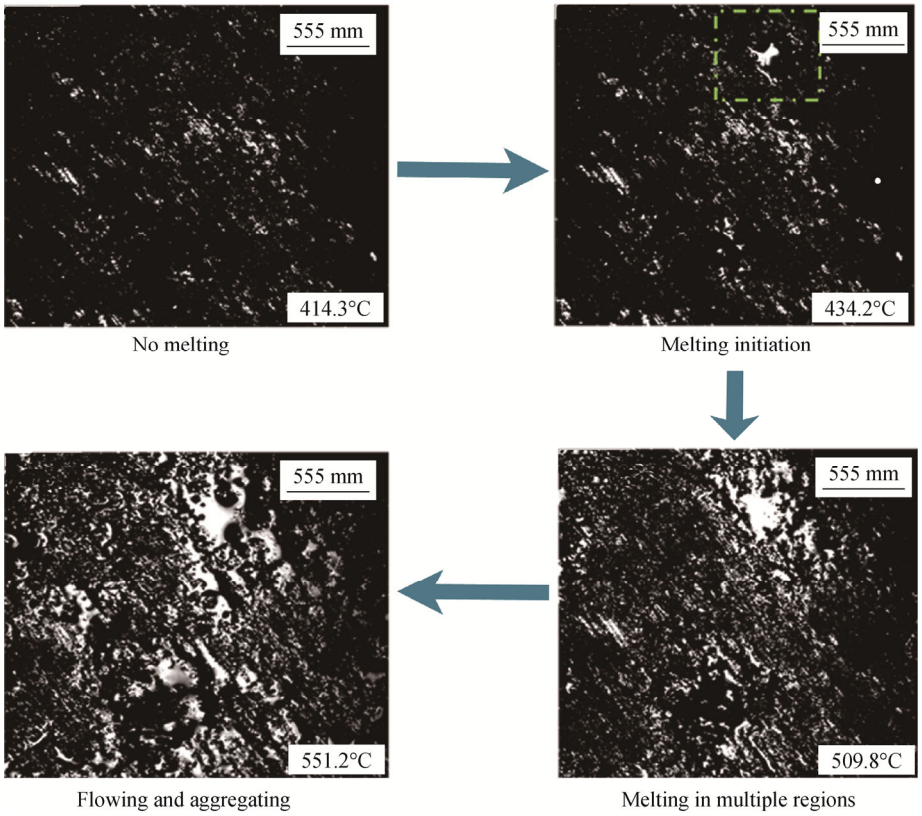

Fig. 16. Melting and aggregation processes of slag.

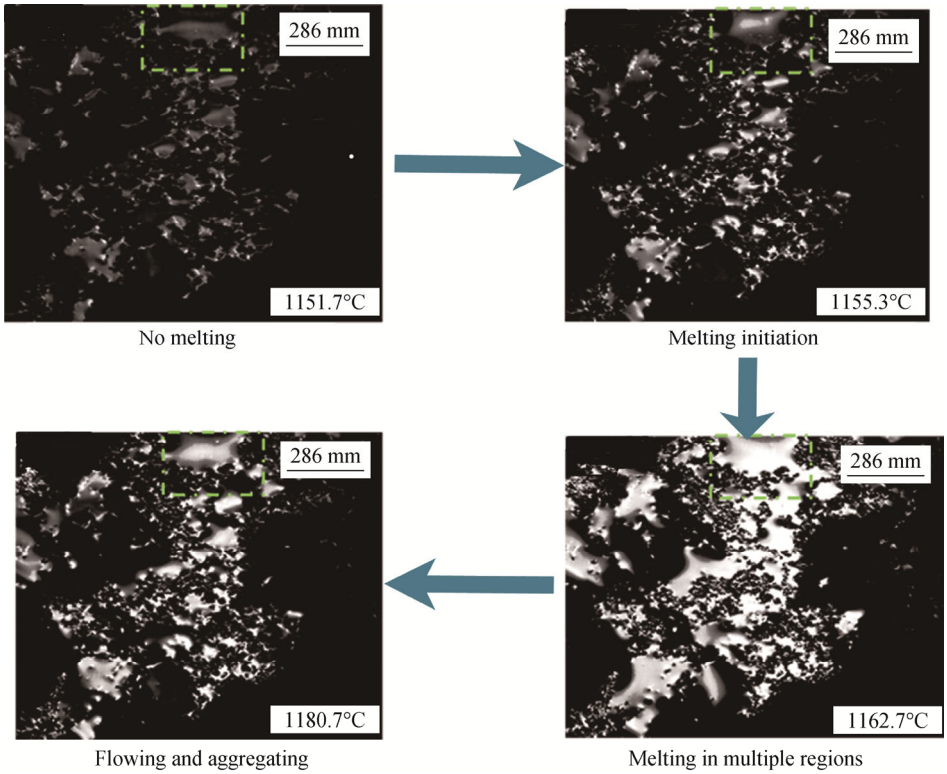

Fig. 17. Melting and aggregation processes of iron.

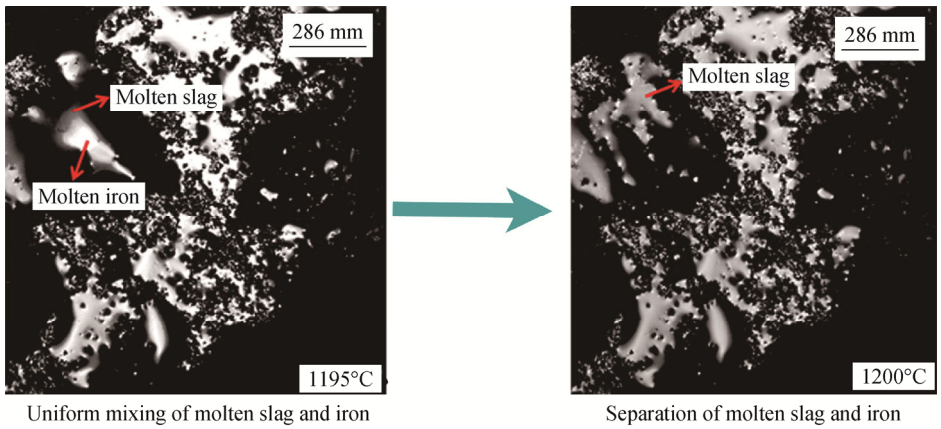

Fig. 18. Separation process of molten slag and iron.

4. Conclusions

In this work, a novel method named "direct reduction–sodium oxidation–smelting separation coupled technology" for the comprehensive utilization of vanadium-bearing titanomagnetite was proposed and investigated. During the roasting process, the direct reduction of iron oxides, sodium oxidation of vanadium oxides to water-soluble sodium vanadate, and slag/iron smelting separation were realized simultaneously. After the roasting process, the water leaching process was used to dissolve the water-soluble sodium vanadate in the roasting slag. Finally, 93.67% iron, 72.68% vanadium, and 99.72% titanium from the raw ore were concentrated in iron nuggets, the vanadium-bearing leaching liquor, and the leaching residue, respectively. The proposed process offers numerous advantages over traditional methods, such as lower energy consumption, a shorter operational circle without production of hazardous materials, and higher resource recovery. This process thus represents a substantial advancement in the comprehensive utilization of vanadium-bearing titanomagnetite. In the future, the extraction of vanadium from the vanadium-bearing leaching liquor and the utilization of the titanium residue will be systematically studied.

Acknowledgements

This work was financially supported by the National Basic Research Program of China (Nos. 2013CB632601 and 2013CB632604), the National Science Foundation for Distinguished Young Scholars of China (Nos. 51125018 and 51504230), the Key Research Program of the Chinese Academy of Sciences (No. KGZD-EW-201-2), the National Natural Science Foundation of China (Nos. 51374191, 21106167, 2160624, and 51104139), the Financial Grant from the China Postdoctoral Science Foundation (Nos. 2012M510552 and 2013T60175), and the Nonprofit Industry Research Subject of Environmental Projection (No. 201509053).

References

[1] C. Li, B. Liang, L.H. Guo, and Z.B. Wu, Effect of mechanical activation on the dissolution of Panzhihua ilmenite, *Miner. Eng.*, 19(2006), No. 14, p. 1430.

[2] X.H. Liu, G.S. Gai, Y.F. Yang, Z.T. Sui, L. Li, and J.X. Fu, Kinetics of the leaching of TiO_2 from Ti-bearing blast furnace slag, *J. China Univ. Min. Technol.*, 18(2008), No. 2, p. 275.

[3] J.L. Wang, Development and utilization for the vanadium-bearing titanomagnetite in oversea areas, *Vanadium Titanium*, 1993, No. 5, p. 1.

[4] Z.H. Wang, Multipurpose utilization of vanadium-bearing titanomagnetite and vanadium and titanium industry, *Vanadium Titanium*, 1993, No. 4, p. 1.

[5] L.H. Zhou, J. Wang, S.Y. Gou, L.Y. Chen, and Z.R. Li, Development of utilization of vanadic titanomagnetite, *Appl. Mech. Mater.*, (2012), No. 184-185, p. 949.

[6] W.G. Fu, Y.C. Wen, and H.E. Xie, Development of intensified technologies of vanadium-bearing titanomagnetite smelting, *J. Iron Steel Res. Int.*, 18(2011), No. 4, p. 7.

[7] L. Zhang, L.N. Zhang, M.Y. Wang, G.Q. Li, and Z.T. Sui, Recovery of titanium compounds from molten Ti-bearing blast furnace slag under the dynamic oxidation condition, *Miner. Eng.*, 20(2007), No. 7, p. 684.

[8] B. Liu, H. Du, S.N. Wang, Y. Zhang, S.L. Zheng, L.J. Li, and D.H. Chen, A novel method to extract vanadium and chromium from vanadium slag using molten NaOH–$NaNO_3$ binary system, *AICHE J.*, 59(2013), No. 2, p. 541.

[9] T.P. Lou, Y.H. Li, J.W. Ma, Y.H. Xia, and Z.T. Sui, The isothermal growth of perovskite phase in the blast furnace slag bearing titania, *Acta Metall. Sin.*, 35(1999), No. 8, p. 834.

[10] K.J. Hu, G. Xi, J. Yao, and X. Xi, Status quo of manufacturing techniques of titanium slag in the world, *World Nonferrous Met.*, 2006, No. 12, p. 26.

[11] X. Xue, Research on direct reduction of vanadic titanomagnetite, *Iron Steel Vanadium Titanium*, 28(2007), No. 3, p. 37.

[12] J. Deng, X. Xue, and G.G. Liu, Current situation and development of comprehensive utilization of vanadium-bearing titanomagnetite at PANGANG, *J. Mater. Metall.*, 6(2007), No. 2, p. 83.

[13] R.R. Moskalyk and A.M. Alfantazi, Processing of vanadium: a review, *Miner. Eng.*, 16(2003), No. 9, p. 793.

[14] L.S. Zhao, L.N. Wang, T. Qi, D.S. Chen, H.X. Zhao, and Y.H. Liu, A novel method to extract iron, titanium, vanadium, and chromium from high-chromium vanadium-bearing titanomagnetite concentrates, *Hydrometallurgy*, (2014), No. 149, p. 106.

[15] Y.M. Zhang, L.Y. Yi, L.N. Wang, D.S. Chen, H.X. Zhao, and T. Qi, A novel process for recovery of iron, titanium, and vanadium from vanadium-bearing titanomagnetite: sodium modification–direct reduction coupled process, *Int. J. Miner. Metall. Mater.*, 24(2016), No. 5, p. 504.

[16] B.Z. Ma, C.Y. Wang, W.J. Yang, F. Yin, and Y.Q. Chen, Screening and reduction roasting of limonitic laterite and ammonia–carbonate leaching of nickel–cobalt to produce a high-grade iron concentrate, *Miner. Eng.*, 50-51(2013), No. 9, p. 106.

[17] H.P. Klug and L.E. Alexander, *X-Ray Diffraction Procedures: for Polycrystalline and Amorphous Materials*, Wiley, New York, 1974.

[18] H.H. Tang, W. Sun, Y.H. Hu, and H.S. Han, Comprehensive recovery of the components of ferritungstite base on reductive roasting with mixed sodium salts, water leaching and magnetic separation, *Miner. Eng.*, (2016), No. 86, p. 34.

[19] A. Lahiri and A. Jha, Kinetics and reaction mechanism of soda ash roasting of ilmenite ore for the extraction of titanium dioxide, *Metall. Mater. Trans. B*, 38(2007), No. 6, p. 939.

[20] K. Tsutsumi, T. Nagasaka, and M. Hino, Surface roughness of solidified mold flux in continuous casting process, *ISIJ Int.*, 39(1999), No. 11, p. 1150.

[21] H.L. Han, D.P. Duan, S.M. Chen, and P. Yuan, Mechanism and influencing factors of iron nuggets forming in rotary hearth furnace process at lower temperature, *Metall. Mater. Trans. B*, 46(2015), No. 5, p. 2208.

[22] J. Lu, S.J. Liu, S.G. Ju, W.G. Du, P. Feng, and Y. Song, The effect of sodium sulphate on the hydrogen reduction process of nickel laterite ore, *Miner. Eng.*, 49(2013), No. 8, p. 154.

[23] W. Yu, T.C. Sun, J. Kou, Y.X. Wei, C.Y. Xu, and Z.Z. Liu, The function of $Ca(OH)_2$ and Na_2CO_3 as additive on the reduction of high-phosphorus olitic hematite–coal mixed pellets, *ISIJ Int.*, 53(2013), No. 3, p. 427.

[24] V.A. Imideev, P.V. Aleksandrov, A.S. Medvedev, O.V. Bazhenova, and A.R. Khanapieva, Nickel sulfide concentrate processing using low-temperature roasting with sodium chloride, *Metallurgist*, 58(2014), No. 5-6, p. 353.

[25] Q. Guo, J.K. Qu, B.B. Han, G.Y. Wei, P.Y. Zhang, and T. Qi,

Dechromization and dealumination kinetics in process of Na_2CO_3-roasting pretreatment of laterite ores, *Trans. Nonferrous Met. Soc. China*, 24(2014), No. 12, p. 3979.

[26] Z. Alizade and K.H. Khalilova, Vanadium oxidation during reducing roasting of titanomagnetite concentrates by natural gas with sodium carbonate present, *Russ. J. Appl. Chem.*, 68(1995), No. 6, p. 785.

[27] X.G. Huang, *Iron and Steel Metallurgy Principle*, Metallurgical Industry Press, Beijing, 2011.

[28] K. Mukai, Interfacial phenomena, metals processing and properties, *Fundam. Metall.*, 2005, No. 2, p. 237.

[29] Z.L. Xue, D. Yang, L.G. Zhou, and Y.Y. Li, Effects of technical factors on iron nuggets separated from slag by Wcomet process, *J. Wuhan Univ. Sci. Technol.*, 32(2009), No. 1, p. 1.

[30] K. Ishizaki, K. Nagata, and T. Hayashi, Production of pig iron from magnetite ore–coal composite pellets by microwave heating, *ISIJ Int.*, 46(2006), No. 10, p. 1403.

[31] H. Ono, K. Tanizawa, and T. Usui, Rate of iron carburization by carbon in slags through carbon/slag and slag/metal reactions at 1723 K, *ISIJ Int.*, 51(2011), No. 8, p. 1274.

[32] K.I. Ohno, A. Babich, J. Mitsue, T. Maeda, D. Senk, H.W. Gudenau, and M. Shimizu, Effects of charcoal carbon crystallinity and ash content on carbon dissolution in molten iron and carburization reaction in iron-charcoal composite, *ISIJ Int.*, 52(2012), No. 8, p. 1482.

[33] P. Villars, A. Prince, and H. Okamoto, *Handbook of Ternary Alloy Phase Diagrams*, ASM International, Materials Park, OH, 1995.

[34] S.T. Cham, R. Khanna, V. Sahajwalla, R. Sakurovs, and D. French, Influence of mineral matter on carbon dissolution from metallurgical coke into molten iron: interfacial phenomena, *ISIJ Int.*, 49(2009), No. 12, p. 1860.